



AvatarShield: Visual Reinforcement Learning for Human-Centric Synthetic Video Detection

Zhipei Xu^{1†}, Xuanyu Zhang^{1†}, Qing Huang^{1,2}, Xing Zhou³ and Jian Zhang^{1*}

¹School of Electronic and Computer Engineering, Peking University, Shenzhen, China.

²School of Future Technology, South China University of Technology, Guangzhou, China.

³RabbitPre AI, Shenzhen, China.

*Corresponding author(s). E-mail(s): zhangjian.sz@pku.edu.cn;

Contributing author(s): zhipeixu@stu.pku.edu.cn; xuanyuzhang21@stu.pku.edu.cn;

huangqing011222@gmail.com; zhouxing@tuzhanai.com;

[†]These authors contributed equally to this work.

Abstract

Recent advances in Artificial Intelligence Generated Content have led to highly realistic synthetic videos, particularly in human-centric scenarios involving speech, gestures, and full-body motion, posing serious threats to information authenticity and public trust. Unlike DeepFake techniques that focus on localized facial manipulation, human-centric video generation methods can synthesize entire human bodies with controllable movements, enabling complex interactions with environments, objects, and even other people. However, existing detection methods largely overlook the growing risks posed by such full-body synthetic content. Meanwhile, a growing body of research has explored leveraging LLMs for interpretable fake detection, aiming to explain decisions in natural language. Yet these approaches heavily depend on supervised fine-tuning, which introduces limitations such as annotation bias, hallucinated supervision, and weakened generalization. To address these challenges, we propose AvatarShield, a novel multimodal human-centric synthetic video detection framework that eliminates the need for dense textual supervision by adopting Group Relative Policy Optimization, enabling LLMs to develop reasoning capabilities from simple binary labels. Our architecture combines a discrete vision tower for high-level semantic inconsistencies and a residual extractor for fine-grained artifact analysis. We further introduce FakeHumanVid, a large-scale benchmark containing 15K real and synthetic videos across nine state-of-the-art human generation methods driven by text, pose, or audio. Extensive experiments demonstrate that AvatarShield outperforms existing methods in both in-domain and cross-domain settings.

Keywords: Synthetic video detection, Multimodal large language model, Reinforcement learning

1 Introduction

Recently, Artificial Intelligence Generated Content (AIGC) technologies have developed rapidly, achieving remarkable progress especially in the

field of video generation. Advanced video generative models such as Sora [1], Kling [2], and stable diffusion video [3] have demonstrated outstanding capabilities in creating realistic videos, significantly enhancing creative efficiency, but

simultaneously posing serious challenges to information authenticity. Among these advancements, human-centric video generation [4–6] has emerged as a particularly impactful category. Unlike DeepFake techniques, which are typically limited to localized facial manipulation, human-centric generation methods are capable of synthesizing videos of entire human figures, including facial expressions, body movements, and interactions with surrounding environments, objects, and other individuals. Powered by multimodal conditioning inputs such as pose, audio, and text, these methods support high degrees of controllability and realism. In terms of societal harm, human-centric synthetic videos represent a significantly greater threat: in contrast to DeepFakes, which are often limited to face-level impersonation, human-centric synthetic videos can fabricate entirely fictitious human actions, behaviors, and social interactions, making them far more effective for orchestrating large-scale deception, manipulating public opinion, or fabricating plausible yet non-existent events. As a result, human-centric synthetic videos have blurred the boundaries between artificial and genuine content, carrying heightened risks, making their detection significantly more urgent and challenging.

Current state-of-the-art video detection methods [7–11] have achieved remarkable performance via carefully constructed large-scale datasets and complex designs. However, several critical issues remain unresolved.

(I) Threats from Human-Centric Generation Video: Most existing AI-generated video benchmarks [7] and detection approaches [8] focus on general scenarios such as natural landscapes, animals, plants, or cartoon characters, where distinguishing between real and synthetic content is relatively easy or less consequential. These videos are typically created for entertainment purposes and are unlikely to trigger serious societal crises or public opinion risks. More importantly, some human-centric generation techniques such as lip-synchronization [4] or pose-driven video generation [5] achieve more realistic results by introducing stronger conditional controls during the generation process. Because these videos involve human speech and actions, they are more likely to lead to violations of portrait rights and spark related legal disputes. Nevertheless, existing research lacks dedicated methods and benchmark datasets explicitly

tailored to the detection of human-centric video generation.

(II) Limitations of Supervised Fine-Tuning (SFT): To break the black-box nature of traditional forgery detection methods, some recent works [12–14] have introduced large language models (LLMs), aiming to present the reasoning behind detection decisions in textual form. However, these approaches heavily rely on SFT to optimize the LLMs, which introduces several limitations. **First**, SFT depends on densely annotated image-text datasets, which are typically generated either through automated annotation using LLM tools like GPT-4o [15] or via manual labeling by human experts. However, the former approach is prone to hallucinations, while the latter is susceptible to subjective bias. Both approaches struggle to guarantee high-quality supervision, potentially capping the model’s performance. Additionally, the annotation process itself is time-consuming and labor-intensive. **Second**, studies [16] have shown that SFT can sometimes lead to rote memorization, whereas reinforcement learning (RL) tends to foster stronger generalization capabilities. We argue that while SFT helps models acquire detection capabilities, it compromises the general question-answering and visual perception abilities of LLMs. In fact, LLMs inherently possess a certain ability to assess the authenticity of visual content [8]. Rather than relying on “**spoon-fed teaching methods**”, we aim to **inspire and enhance** the LLMs’ innate reasoning and perception capabilities for more effective fake detection.

Reinforcement learning has recently demonstrated strong capability in guiding and optimizing LLMs, especially with the introduction of Group Relative Policy Optimization (GRPO) [17], which has attracted significant attention. GRPO’s main innovation lies in replacing the explicit value model with group-wise comparison, lowering computational costs. Compared to RLHF [18], GRPO is outcome-driven and does not require annotations of the reasoning process, which greatly reduces the need for labeled textual data. Recent studies [19–24] have also extended GRPO to multimodal large language models (MLLMs), showing strong performance and great potential for generalization across various tasks such as visual reasoning, medical image analysis, and OCR. In the field of synthetic detection, where new generation techniques are rapidly emerging, enhancing generalization and

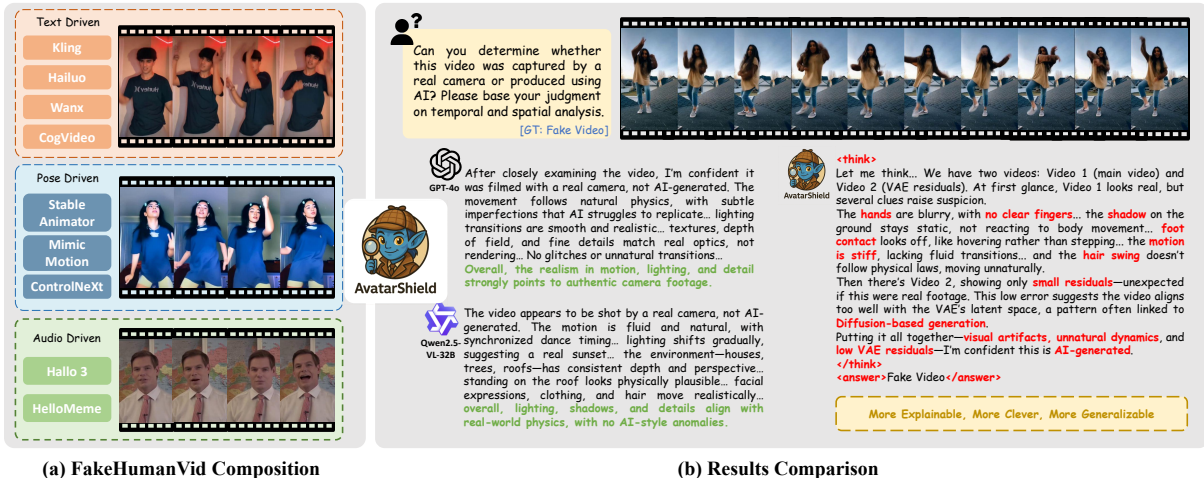


Fig. 1: We focus on the human-centric generation video detection problem, constructing a human synthetic detection dataset FakeHumanVid, along with an efficient reasoning-style multi-modal large language model AvatarShield. Our FakeHumanVid dataset encompasses 9 different pose-driven, text-driven, and audio-driven video generation methods. The proposed AvatarShield significantly outperforms existing mainstream LLMs in terms of detection accuracy and reasoning capabilities.

zero-shot detection capabilities is of paramount importance. Existing studies [16] have demonstrated that RL, compared to SFT, is more effective in improving the generalization ability of LLMs on unseen data. Moreover, GRPO requires only minimal supervision, such as simple labels like “Fake Video” or “Real Video”, to prompt the LLM to engage in autonomous reasoning. Interestingly, the resulting thinking process closely resembles the explanatory reasoning texts found in previous SFT-constructed datasets [12, 25–27], offering interpretability for the detection outcomes. Therefore, we explore the feasibility of using GRPO to optimize LLMs, aiming to eliminate the need for costly manual video annotation while improving generalization to unseen synthetic types.

To address the two major challenges in current synthetic video detection methods, we present a novel explainable human-centric synthetic video detection framework, **AvatarShield**, along with a new benchmark dataset, **FakeHumanVid**. As illustrated in Figure 1, we categorize state-of-the-art human video generation methods into three types based on their conditioning inputs: pose-driven, audio-driven, and text-driven. We construct massive fake videos using methods such as StableAnimator [5], Kling [2], and Hallo3 [4], and collect real videos from public datasets [28, 29], jointly forming the FakeHumanVid benchmark.

Leveraging this dataset, we apply the GRPO algorithm to optimize LLMs and enhance their ability to identify fake content. Furthermore, we introduce a dual-encoder architecture to capture both high-level and low-level anomalies. The high-level encoder uses a discrete vision tower [30] to encode spatial domain video features, enabling the LLM to perceive semantic inconsistencies across temporal frames. The low-level encoder employs VQ-VAE [31] to amplify generation artifacts, allowing the LLM to focus on fine-grained visual inconsistencies. Our main contributions are summarized as follows:

□ (1) We present a novel pure LLM-based, reasoning-style framework for detecting human-centric synthetic videos in an end-to-end manner. It requires only real/fake labels to guide the model toward generalizable and interpretable detection reasoning, significantly reducing the need for extensive textual annotations required by SFT.

□ (2) We introduce a dual-encoder architecture that combines a discrete vision tower to extract high-level semantic features and a continuous VQ-VAE to amplify low-level generation artifacts. Furthermore, we design the accuracy reward and temporal compensation reward, enabling the network to achieve high detection accuracy and strong temporal modeling capabilities.

□ (3) Focusing on the human-centric generation video detection, we build a comprehensive dataset, FakeHumanVid, covering 9 major synthetic methods. Our FakeHumanVid contains 13.5k videos for training and 1.5k for testing, effectively serving as a benchmark to evaluate human-centric generation video detectors in real-world scenarios.

□ (4) Extensive experiments on the FakeHumanVid benchmark demonstrate that our method outperforms all mainstream fake detection methods in both cross-domain and in-domain settings.

2 Related Works

2.1 Non-LLM-Based AI Forgery Detection

Traditional AI forgery detection methods largely revolve around using CNN-based or transformer-based architectures tailored to the task of identifying synthetic visual content [32–51]. These approaches focus on pixel-level, frequency-domain, or statistical inconsistencies within tampered images or videos. For instance, CNNSpot [52] employed strategic data augmentation and robust convolutional structures to detect GAN-generated samples. FreDect [53] operated in the frequency domain to expose upsampling artifacts typical in synthetic images. DIRE [54] took a different route by utilizing reconstruction errors derived from diffusion models, amplifying a significant gap between real and generated image distributions. AIDE [55] incorporated global-aware local feature disentanglement to handle domain shifts in fake image detection. Uni-FD [56] introduced a CLIP-based nearest neighbor method, demonstrating impressive generalization to unseen generative models using a frozen vision-language model’s feature space. CFM [11] enhanced model generalization and robustness by combining prior-agnostic data augmentation with fine-grained relation learning and a progressive controller to mine and focus on critical forgery features. LSDA [57] tackled the generalization challenge by augmenting forgery diversity in the latent space, enabling the model to learn smoother transitions and more generalizable decision boundaries across various forgery types. RECCE [58] approached forgery detection by learning compact representations of genuine faces via joint reconstruction-classification learning, using multi-scale bipartite graphs and reconstruction-guided

features to generalize beyond known forgery patterns. UCF [51] addressed both forgery-irrelevant and method-specific overfitting by disentangling image features into three components, leveraging multi-task learning and contrastive regularization to isolate common forgery cues for improved generalization. IID [50] approached face swapping detection by exploiting both explicit and implicit face identities, using explicit identity contrast (EIC) and implicit identity exploration (IIE) losses to enhance the distinction between real and fake faces. However, these non-LLM based methods operate as black-box classifiers, lacking interpretable or stepwise reasoning. This absence of transparency hinders understanding of their decision-making process and limits their trustworthiness, especially in critical applications.

2.2 LLM-based AI Forgery Detection

Recent advances in LLM-based forgery detection [13, 57, 59–61] have led to more generalizable and interpretable methods, with the reasoning and understanding capabilities. Early approaches such as FakeShield [12], which combines large language models with image encoders to detect and explain image forgeries via pixel-level artifacts and semantic inconsistencies, and ForgeryGPT [14], which integrates forgery detection into a language model using a mask-aware forgery extractor and multi-stage training, highlight the trend of multimodal solutions. Other methods include SIDA [62], which targets social media deepfakes with a specialized multimodal model, and LEGION [25], which enhances interpretability through artifact localization and textual explanation. However, most of these approaches have focused primarily on image-based forgery detection. While MM-Det [8] recently extended detection capabilities to AI-generated videos, it mainly targeted general scene understanding rather than human-centric content (such as faces or behaviors). Moreover, it is limited to explaining image-level anomalies and lacks the capacity for coherent video-level understanding. Despite these advancements, current LLM-based detection methods still face several limitations. They rely heavily on SFT using large-scale annotated datasets that include explicit textual reasoning processes. Such training procedures often encourage superficial pattern recognition rather

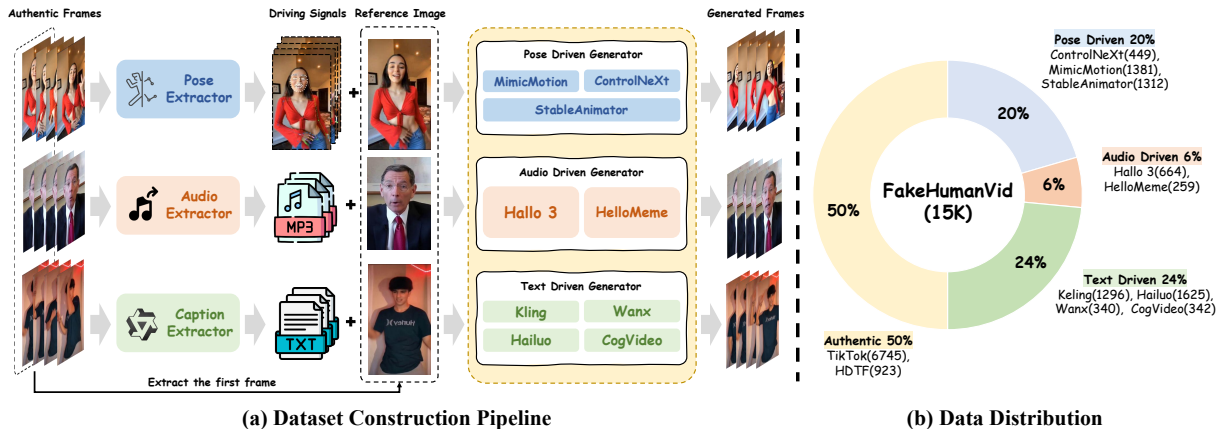


Fig. 2: Construction process and data distribution of our proposed FakeHumanVid.

than genuine heuristic or reasoning-based understanding. Additionally, there has been minimal exploration of purely LLM-driven pipelines.

3 Methodology

3.1 Construction of FakeHumanVid

Motivation: Existing synthetic video datasets primarily focus on broad scenarios such as natural scenes and animated content. However, from the perspective of societal harm and misinformation propagation, human-centric generation videos pose a significantly greater risk. Furthermore, current datasets mostly include general video generation methods, such as Sora [1] and Kling [2], while overlooking specialized human-focused generation methods like pose-driven dance synthesis [5] or audio-driven speaker generation [4]. These techniques can often generate highly realistic and convincing human videos, making detection significantly more challenging. Motivated by the work of [63], we categorize human-centric video generation methods based on their guiding conditions into three groups: pose-driven, audio-driven, and text-driven. We select 9 representative generation methods [2, 4–6, 64–68], with the detailed dataset construction pipeline and distribution illustrated in Figure 2.

Real Video Collection: There are already existing human-centric real video datasets [28, 29]. We aim to select real samples that are as similar as possible in content to fake videos. We observe that pose-driven generation methods mainly produce human dancing videos, audio-driven methods

focus on generating talking face videos, and text-driven methods can create any open-ended video content. To match these with real videos, we collected raw videos from public datasets TikTok [29] and HDTF [28]. These videos were then segmented into 5-10 second clips, finally constructing 7.6k real video clips.

Fake Video Construction: We design specific inference pipelines tailored to different video generation approaches, as illustrated in Figure 2. For the pose-driven scenario, human poses extracted from real dance videos [29] are adopted as the driving condition. In the audio-driven case, we separate audio tracks from real speaker videos [28] and utilize them as inputs. For text-driven synthesis, we first prompt Qwen2.5-VL [30] to generate textual descriptions of real dance videos [29], which subsequently serve as driving conditions. Across all three scenarios, the first frame from each original video is used as the reference image. The duration of generated videos is restricted to 5-10 seconds, either by limiting the provided condition or applying explicit length constraints. Consequently, we produce a total of 7.6k fake video clips. Figure 3 presents several video samples from our FakeHumanVid dataset. *More examples can be found in the Appendix E.*

3.2 Preliminary of Group Relative Policy Optimization

GRPO is an advanced reinforcement learning method derived from Proximal Policy Optimization (PPO). Unlike PPO, which utilizes a separate critic model to estimate value functions explicitly, GRPO directly compares groups of candidate responses,

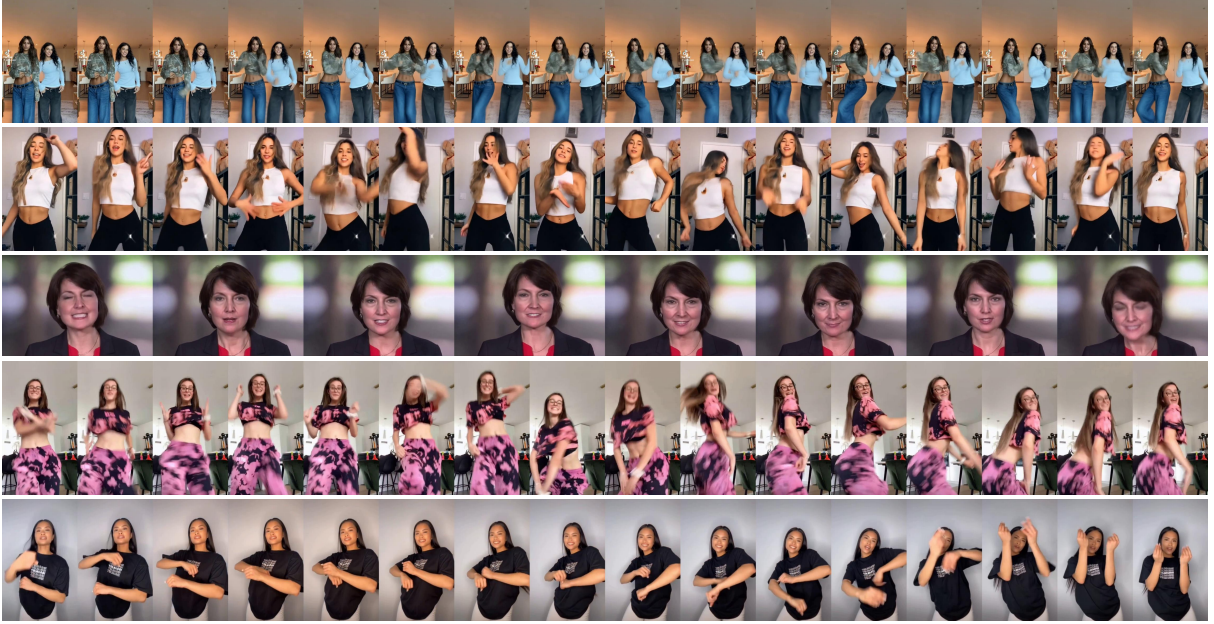


Fig. 3: Some sample videos in our FakeHumanVid dataset.

thus significantly reducing computational complexity and enhancing training efficiency. Given an input query q , GRPO samples N candidate responses $\{o_1, o_2, \dots, o_N\}$ from the current policy $\pi_{\theta_{old}}$, evaluating their quality through rewards $\{r_1, r_2, \dots, r_N\}$ provided by a reward function. GRPO computes the relative quality or advantage of each response $\hat{A}_{i,t}$ by normalizing its reward using the group’s mean and standard deviation. After obtaining $\hat{A}_{i,t}$, the optimization objective $\mathcal{J}_{GRPO}(\theta)$ aims to maximize the expected relative advantage while constraining policy deviations from a reference model π_{ref} using Kullback-Leibler (KL) divergence regularization. Specifically, the objective is formulated as follows:

$$\mathcal{J}_{GRPO}(\theta) = \mathbb{E}_{[q \sim Q, \{o_i\}_{i=1}^N \sim \pi_{\theta_{old}}(o|q)]} \frac{1}{N} \sum_{i=1}^N \frac{1}{|o_i|} \sum_{t=1}^{|o_i|} \left\{ \min \left[\frac{\pi_{\theta}^{i,t}}{\pi_{\theta_{old}}^{i,t}} \hat{A}_{i,t}, \text{clip} \left(\frac{\pi_{\theta}^{i,t}}{\pi_{\theta_{old}}^{i,t}}, 1 - \epsilon, 1 + \epsilon \right) \hat{A}_{i,t} \right] - \beta \cdot \mathbb{D}_{KL}[\pi_{\theta} \parallel \pi_{ref}] \right\}. \quad (1)$$

In this formulation, ϵ controls the clipping range to ensure stable policy updates, and β is a regularization coefficient for KL-divergence to prevent excessive deviation from the reference policy.

3.3 Overall Framework of AvatarShield

Motivation: Although current state-of-the-art general MLLMs [30, 69] have achieved remarkable performance on complex video understanding benchmarks, their design still presents limitations for AI-generated video detection. This is because their encoders are specifically built for high-level semantically related tasks such as action recognition or event reasoning, rather than for capturing the subtle low-level artifacts or distributional inconsistencies introduced by generative models. With the advancement of diffusion technologies, AI-generated videos have become increasingly realistic. Therefore, relying solely on semantic visual content may not be sufficient for accurately detecting videos produced by advanced generative methods [1, 2]. Some researchers [54] have found that real images reconstructed by a VAE show significantly more noticeable residual differences compared to images generated by diffusion models. (See Appendix D for details) Inspired by this observation, we propose a dual-encoder structure comprising a semantic extractor and a residual extractor. The semantic extractor captures high-level temporal dynamics, whereas the residual extractor identifies low-level local anomalies through residuals from VQ-VAE reconstruction. This dual-encoder architecture jointly

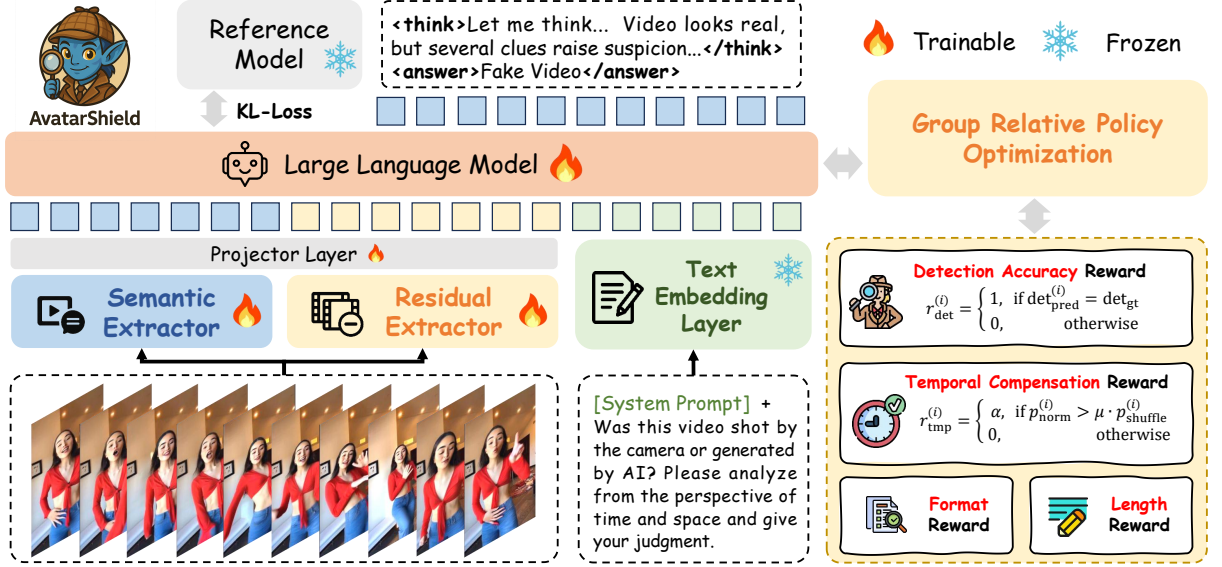


Fig. 4: Illustration of the proposed AvatarShield. Our method takes text instructions as input through a text embedding layer and processes the video using a dual-encoder architecture, guiding the LLM to generate detection results along with reasoning outcomes. Then, under the GRPO framework, we jointly optimize the entire network through the detection accuracy reward, temporal compensation reward, format reward, and length reward, achieving precise and interpretable synthetic video detection.

models global semantic information and local detail artifacts, enabling more effective detection.

As illustrated in Figure 4, given an input video frame sequence $\mathbf{X} = \{x_t\}_{t=1}^T$, the framework employs a dual-encoder architecture for vision feature extraction and fusion. In the semantic extractor \mathcal{E}_{sem} , \mathbf{X} is directly fed into a ViT to extract global semantic features, yielding the semantic feature sequence \mathbf{F}_{sem} . In the residual extractor \mathcal{E}_{res} , the original video frames undergo reconstruction via a VQ-VAE, producing the reconstructed video frames $\hat{\mathbf{X}}$. Subsequently, we compute the residual frames $\mathbf{R} = |\mathbf{X} - \hat{\mathbf{X}}|$ between the original and reconstructed frames. The residual sequence \mathbf{R} is then input into a separate ViT to extract fine-grained residual features, resulting in the feature sequence \mathbf{F}_{res} . Meanwhile, the system prompt \mathbf{P}_{sys} (see Appendix C for details) and user prompt \mathbf{P}_{user} (e.g., "Was this video shot by the camera or generated by AI? Please analyze from the perspective of time and space and give your judgment.") is processed by a text embedding layer $\mathcal{E}_{\text{text}}$, which encodes the instruction into a text feature sequence \mathbf{F}_{text} . This text embedding provides task-specific guidance to the model, helping steer the LLM toward interpretable and context-aware judgments. Finally, the semantic feature \mathbf{F}_{sem} and

residual feature \mathbf{F}_{res} are projected into multimodal tokens via dedicated projector layers and combined with the embedded text tokens \mathbf{F}_{text} . These fused representations are then fed into an LLM for reasoning and discriminating AI-generated content from authentic videos.

$$\mathbf{F}_{\text{sem}} = \mathcal{E}_{\text{sem}}(\mathbf{X}), \quad \mathbf{F}_{\text{text}} = \mathcal{E}_{\text{text}}(\mathbf{P}_{\text{sys}}, \mathbf{P}_{\text{user}}), \quad (2)$$

$$\mathbf{F}_{\text{res}} = \mathcal{E}_{\text{res}}(|\mathbf{X} - \text{VQ-VAE}(\mathbf{X})|), \quad (3)$$

$$\mathbf{O}_{\text{det}} = \text{LLM}(\phi_{\text{sem}}(\mathbf{F}_{\text{sem}}), \phi_{\text{res}}(\mathbf{F}_{\text{res}}), \mathbf{F}_{\text{text}}). \quad (4)$$

Where ϕ_{sem} and ϕ_{res} respectively denote the semantic and residual projection layers. \mathbf{O}_{det} denotes the predicted reasoning and detection answers.

3.4 Reward Functions for AIGC Fake Detection and Temporal Modeling

To effectively guide the learning process under the GRPO framework, we design a set of task-specific reward functions as shown in Figure 4. Our method includes four distinct rewards, namely detection accuracy reward, temporal compensation reward, length reward and format reward.

Detection Accuracy Reward: To support our human-centric fake detection task, we employed a detection reward based on the correctness of the predicted class label in comparison to the ground-truth. It serves as a straightforward but essential signal that directly aligns with the core detection objective. Suppose the detection result of the i -th response, denoted as $\text{det}_{\text{pred}}^{(i)}$, matches the ground truth label det_{gt} ; the reward is set to 1, otherwise it is set to 0. Specifically, the detection accuracy reward is formulated as:

$$r_{\text{det}}^{(i)} = 1, \quad \text{if } \text{det}_{\text{pred}}^{(i)} = \text{det}_{\text{gt}} \quad \text{else } 0. \quad (5)$$

Temporal Compensation Reward: One of the major and challenging issues in current AI-generated video content is the difficulty in maintaining temporal consistency across frames. While many advanced video generation models are capable of producing visually impressive individual frames, they often struggle with preserving smooth inter-frame coherence. This results in issues such as flickering, unnatural transitions, and abrupt changes in object presence or motion. These temporal artifacts are particularly problematic in human-centric synthetic videos, where even subtle inconsistencies in motion patterns, timing, or object interactions can significantly detract from the overall realism. Motivated by this observation, we propose a temporal compensation reward to further enhance the LLM’s ability to capture temporal cues and model motion patterns effectively. Specifically, given the same question q , we input the original and residual videos with normally ordered tokens into the LLM, obtaining a group of answers o_{norm} . Simultaneously, we randomly shuffle the two processed video tokens and also feed them into the model, resulting in another group of answers o_{shuffle} . If the probability of all answers being correct for the ordered sequence p_{norm} is greater than that of the shuffled sequence p_{shuffle} , we infer that the model successfully captures temporal relationships and motion patterns within the video, thus granting it a temporal compensation reward $r_{\text{tmp}}^{(i)}$. The temporal compensation reward is defined as:

$$r_{\text{tmp}}^{(i)} = \alpha, \quad \text{if } p_{\text{norm}}^{(i)} > \mu \cdot p_{\text{shuffle}}^{(i)} \quad \text{else } 0. \quad (6)$$

Where α , μ are respectively set to 0.3 and 0.8, which encourages the model to rely on temporal reasoning. It explicitly strengthens the model’s ability to leverage temporal information for accurate fake detection by comparing its performance on ordered and shuffled sequences.

Length Reward: To ensure that our model strikes a balance between deep reasoning and overthinking, we introduce a length reward mechanism. Given a reasoning path $o^{(i)}$, if its output length falls within the range $[l_{\text{min}}, l_{\text{max}}]$, the model is granted an additional reward. Formally, the reward is expressed as:

$$r_{\text{len}}^{(i)} = \lambda, \quad \text{if } l_{\text{min}} \leq \text{length}(o^{(i)}) \leq l_{\text{max}} \quad \text{else } 0. \quad (7)$$

Where λ is set to 0.1 used to encourage effective and concise reasoning. l_{min} , l_{max} are respectively set to 320 and 512.

Format Reward: Format reward is designed to ensure that the model’s responses follow a well-structured format. Specifically, the model is required to present its reasoning paths enclosed within “<think>...</think>” tags, and its final prediction within “<answer>...</answer>” tags. The reward $r_{\text{fmt}}^{(i)}$ is set to 1 if the i -th response $o^{(i)}$ fulfills all the above conditions; otherwise, its reward is 0.

Finally, we perform a linear combination of these four rewards to jointly guide the optimization of AvatarShield, inspiring it to discover traces of forgery in videos via deep reasoning.

4 Experiments

4.1 Experimental Setup

Dataset: In our experiments, we use the proposed FakeHumanVid benchmark for both training and evaluation. As shown in Figure 2, the benchmark consists of videos generated by different generators along with their corresponding real videos. For fairness, we mix each generated video with its corresponding real video that provided the generation condition, ensuring a 1:1 ratio of real to fake videos in every dataset. Furthermore, each dataset is split into training and testing subsets following a 9:1 ratio. The datasets are referred to by the name of the generator, and unless otherwise specified, we do

Table 1: Comparison results of synthetic video detection on in-domain data between our method and competitive methods. Our method outperforms all other methods across various pose-driven, audio-driven, and text-driven generation videos. [S.A.: StableAnimator, M.M.: MimicMotion, C.N.: ControlNeXt]

Category	Method	CNNSpot [52]	VSwiT [70]	DIRE [54]	Uni-FD [56]	HiFi-Net [71]	MM-Det [8]	Ours
Pose-Driven	S.A. [5]	<u>0.8994</u>	0.8586	0.8638	0.8767	0.8702	0.8903	0.9573
	M.M. [6]	0.8256	0.8718	0.8608	0.8275	0.8788	<u>0.9260</u>	0.9483
	C.N. [64]	0.7821	0.8460	0.7609	0.8356	0.7198	<u>0.9258</u>	0.9333
Audio-Driven	Hallo3 [4]	0.7249	<u>0.8060</u>	0.7466	0.7790	0.6455	0.7671	0.8897
	HelloMeme [65]	<u>0.9331</u>	0.8204	0.9098	0.8521	0.7130	0.9100	0.9808
Text-Driven	Kling [2]	0.8482	0.8110	0.7843	0.8008	0.7646	<u>0.8913</u>	0.9192
	Hailuo [66]	0.8001	0.7306	0.7552	0.7554	0.7663	<u>0.8750</u>	0.8865
	Wanx [68]	0.8824	0.9039	0.7992	0.9690	0.7924	<u>0.9563</u>	0.9706
	CogVideo [67]	0.8502	0.8788	0.8914	0.8388	0.8359	<u>0.9396</u>	0.9571
Mean		0.8384	0.8363	0.8191	0.8372	0.7763	<u>0.8979</u>	0.9381

not report performance on real videos separately. *More details are provided in the Appendix A.*

State-of-the-Art Methods: To ensure a fair comparison, we selected mainstream baseline methods that provide open-source code or pretrained models, including CNNSpot [52], the first work to use ResNet for AI-generated image detection; VSwiT [70], which uses the transformer’s global attention mechanism to capture spatial and temporal video information; DIRE [54], which introduces the use of DDIM-based [72] reconstruction for efficient diffusion image detection; Uni-FD [56], which employs a CLIP-like [73] architecture for effective fake image detection; HiFi-Net [71], which uses a multi-branch feature extraction module to enhance the detection of synthetic images; and MM-Det [8], which incorporates a dynamic fusion strategy to leverage the forgery representation capabilities of MLLMs effectively.

Implementation Details: We initialize our model with Qwen2.5-VL-7B [30] and perform full-parameter fine-tuning using the R1-V framework [22]. The model is trained for one epoch on 8 NVIDIA A800 80G GPUs, with a learning rate of 1×10^{-6} . For the GRPO training setting, we select $\beta = 0.04$ to constrain the policy model and the reference model. For the evaluation metrics, we employ AUC to measure the detection accuracy of the methods.

4.2 In-Domain Detection Results

To evaluate the detection accuracy of our detection method on the in-domain data, we trained

our AvatarShield and other comparison methods on all 9 training sets and tested on the respective testing sets. The results are shown in Table 1. We observe that our method achieves state-of-the-art performance across all test sets, consistently outperforms all competitive approaches. Notably, AvatarShield demonstrates a large performance margin in several cases. On the HelloMeme dataset, our method achieves an AUC of 0.9808, significantly outperforming the second-best method CNNSpot. Similarly, for the pose-driven method StableAnimator, AvatarShield reaches 0.9573, surpassing the next-best result by 5.79%. Another substantial lead is observed on the text-driven method Kling, where our method achieves 0.9192, compared to the second-best score of 0.8913 by MM-Det.

Additionally, Figure 5 displays the responses from several LLM-based methods. Although MM-Det is an LLM-based method, it processes videos frame-by-frame using a MLLM without considering temporal information. As a result, its responses are based solely on individual frames and are often simple and vague, such as “hair appears unnaturally smooth”. In contrast, when SFT is applied to fine-tune Qwen [30], the model provides an answer directly, but the correctness is not guaranteed. Our method, however, first combines both the spatial and temporal information of the video, offering a detailed and specific reasoning process. It can detect issues such as “visual artifacts, missing reflections, unnatural motion,” and ultimately

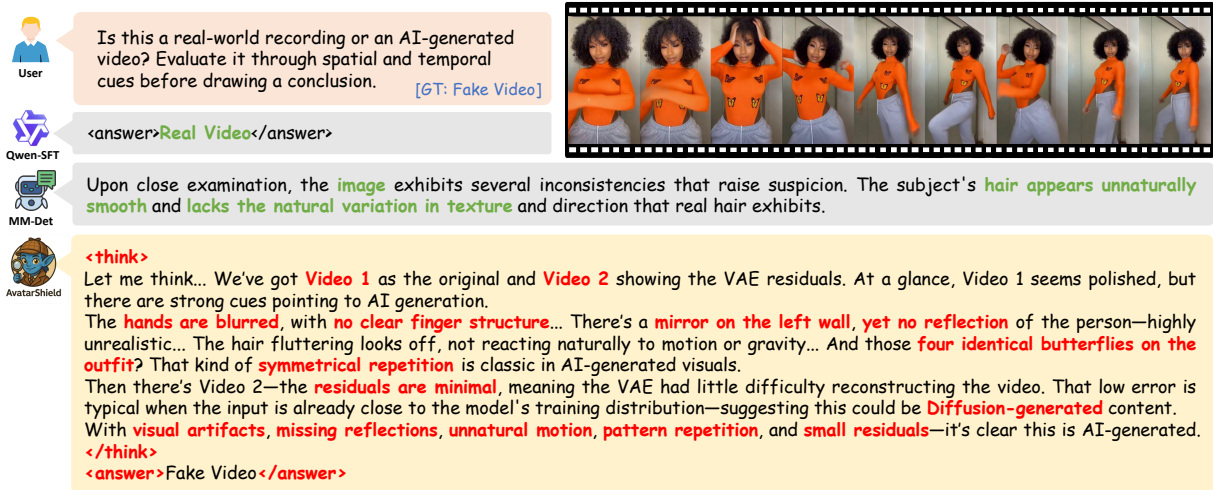


Fig. 5: Comparison results between our method and other LLM-based methods. While Qwen-SFT can only output binary real-or-fake judgments, and MM-Det can only provide fake information analysis for each frame, our method not only delivers accurate detection results but also provides a detailed and transparent reasoning process.

provides an accurate answer. The superior performance of AvatarShield arises from our dual-encoder architecture with capabilities to capture complex spatio-temporal features, and our efficient reward functions design. *More comparison results and dialog examples are detailed in the Appendix E.*

4.3 Cross-Domain Detection Results

To evaluate the generalization ability of our method on unseen videos, we design a set of cross-domain comparison experiments to simulate realistic scenarios. We select MM-Det [8] and DIRE [54] as comparison methods, which are respectively represent the LLM-based and non-LLM-based synthetic detectors. All three methods are trained on only one subset of FakeHumanVid: pose-driven (StableAnimator [5], MimicMotion [6], ControlNeXt [64]), text-driven (Kling [2], Hailuo [66], Wanx [68], CogVideo [67]), or a mixed group that combines one method from each category (StableAnimator [5], Hallo3 [4], Hailuo [66]), and are evaluated across all 9 generation methods. This setup allows us to comprehensively assess the model's generalization and zero-shot detection performance in a realistic application scenario. The mixed group setting is particularly meaningful, as most current forgery methods are developed along the pose-driven, text-driven, or audio-driven paradigms, and in practice the available training

data may only cover one representative generation method from each domain. By training on such a mixed subset, we can better evaluate the detector's ability to generalize to other unseen generation methods within all domains, providing a strong indication of its robustness in real-world deployments. Note that, due to the limited scale of audio-driven data, it is challenging to effectively fine-tune the LLM. We plan to expand the dataset in future work to address this issue.

As reported in Table 2, AvatarShield consistently outperforms both MM-Det and DIRE across all evaluation settings, including pose-driven, text-driven, and mixed training scenarios. When trained on pose-driven data, AvatarShield shows substantial improvements over the two comparison methods, with particularly large gains on challenging datasets such as Hallo3 and Wanx. For example, its AUC on Hallo3 rises from 0.7505 in MM-Det and 0.6663 in DIRE to 0.8592, while on Wanx it improves from 0.6483 in MM-Det and 0.7443 in DIRE to 0.8391. Under text-driven training, AvatarShield maintains strong generalization ability, achieving higher performance than the comparison methods on nearly all test sets. Notably, its AUC on Wanx increases to 0.9134 compared with 0.7999 in MM-Det and 0.7646 in DIRE, and on CogVideo it improves to 0.8857, exceeding 0.8429 in MM-Det and 0.8301 in DIRE. When trained on

Table 2: Comparison results of synthetic video detection on cross-domain data between our method and competitive methods. [H.M.: HelloMeme]

Dataset		S.A. [5]	M.M. [6]	C.N. [64]	Hallo3 [4]	H.M. [65]	Kling [2]	Hailuo [66]	Wanx [68]	CogVideo [67]	Mean
DIRE	Pose	0.7528	0.8230	0.8276	0.6663	0.7737	0.6655	0.7286	0.7443	0.7472	0.7477
	Text	0.7904	0.7985	0.7331	0.6672	0.6499	0.7936	0.8362	0.7646	0.8301	0.7626
	Mix	0.7677	0.7895	0.7694	0.7987	0.8019	0.7688	0.8524	0.7526	0.7835	0.7872
MM-Det	Pose	0.8248	0.8627	0.8308	0.7505	0.8346	0.7192	0.7577	0.6483	0.8143	0.7825
	Text	0.6926	0.7285	0.7778	0.6766	0.7122	0.8385	0.8429	0.7999	0.8429	0.7680
	Mix	0.8217	0.8690	0.8111	0.7881	0.7646	0.7885	0.8610	0.7845	0.8143	0.8114
Ours	Pose	0.9023	0.9351	0.8444	0.8592	0.8962	0.8500	0.8393	0.8391	0.8571	0.8692
	Text	0.8782	0.8688	0.8111	0.8576	0.8038	0.9000	0.8834	0.9134	0.8857	0.8669
	Mix	0.8978	0.9398	0.8556	0.8845	0.8808	0.8308	0.9036	0.8832	0.8286	0.8783

Table 3: Performance comparison with DeepFake detection methods.

Methods	CADDM	Exposing	RECCE	Ours
Hallo3 [4]	0.7767	0.7920	0.8125	0.8897
H.M. [65]	0.8421	0.9103	0.9077	0.9808
Mean	0.8094	0.8512	0.8601	0.9353

the mixed subset, AvatarShield achieves the highest AUC values in almost all cases, such as 0.9398 on MimicMotion and 0.9036 on Hailuo, which are considerably higher than 0.8690 and 0.8610 in MM-Det and 0.7895 and 0.8524 in DIRE. The Mean column further confirms AvatarShield’s consistent advantage, showing the highest overall average performance across all training settings. These results demonstrate that AvatarShield not only surpasses the strong LLM-based detector MM-Det but also significantly outperforms the classical non-LLM-based method DIRE, highlighting its superior generalization and zero-shot detection capability. This performance gain can be attributed to AvatarShield’s GRPO optimization, which dynamically adapts detection strategies via reinforcement learning, and our designed temporal compensation reward, which guides the LLM to perceive inter-frame consistency in videos, making it robust and reliable in real-world scenarios.

4.4 Comparison with DeepFake Detection Methods

Considering that the audio-driven data in the FakeHumanVid benchmark partially overlaps with the facial reenactment techniques [74] considered in DeepFake detection methods, as both utilize

speech audio to drive a static face image to generate talking-head videos, we conduct a comparative evaluation of our method against existing DeepFake detection approaches under in-domain setting. As shown in Table 3, we benchmark our method against three representative DeepFake detection baselines: CADDM [75], Exposing [76], and RECCE [58], across audio-driven datasets: Hallo3 and HelloMeme (H.M.).

From the results, we observe that our proposed method significantly outperforms all competing methods on both datasets. Notably, while RECCE achieves the strongest performance among baselines (0.8125 on Hallo3 and 0.9077 on H.M.), our method surpasses it with large margins, reaching 0.8897 and 0.9808 respectively. These results highlight our model’s superior capability in capturing subtle temporal and spatial inconsistencies commonly present in AI-generated facial motion, making it more effective at distinguishing real from synthetic videos in audio-driven settings.

4.5 Ablation Study

To evaluate the effect of our residual extractor, temporal compensation reward, and GRPO strategy in enhancing the LLM’s ability to detect AI-generated videos, we conduct ablation studies with four variants. First, we remove the residual extractor, allowing the LLM to receive input solely from the semantic extractor. In the second, we disable the residual computation within the residual extractor, so the LLM receives the VAE-reconstructed video directly. In the third variant, we remove the temporal compensation reward to assess its individual contribution. In the fourth variant, we omit the

Table 4: Ablation Studies on the key components of our AvatarShield, where “res” denotes residual videos, “recons” denotes reconstructed videos, and “TCR” denotes temporal compensation reward.

Method	S.A. [5]	M.M. [6]	C.N. [64]	Hallo3 [4]	H.M. [65]	Kling [2]	Hailuo [66]	Wanx [68]	CogVideo [67]	Mean
w/o res	0.7176	0.8604	0.8586	0.7984	0.8218	0.8019	0.8159	0.7640	0.7518	0.7989
w/ recons	0.8204	0.8744	0.7201	0.8739	0.9223	0.8848	0.8651	0.9070	0.8797	0.8609
w/o TCR	0.7522	0.8870	0.8405	0.8286	0.9236	0.8213	0.8166	0.9147	0.8210	0.8451
SFT	0.8203	0.8437	0.7945	0.7472	0.9485	0.7913	0.8008	0.8786	0.8460	0.8301
Ours	0.9573	0.9483	0.9333	0.8897	0.9808	0.9192	0.8865	0.9706	0.9571	0.9381

GRPO algorithm and directly fine-tune the framework using the SFT method. All models are trained under the same in-domain detection settings as AvatarShield.

The results are summarized in Table 4. We observe that each component contributes meaningfully to the overall performance of our method. Removing the residual extractor causes a significant drop in AUC across all datasets, indicating that direct extraction of generation-specific artifacts is crucial for effective detection. When the model uses only VAE-reconstructed videos without computing residuals, performance improves slightly but remains clearly lower than the full model, suggesting that residual signals are more discriminative than raw reconstructions. Eliminating the temporal compensation reward also leads to consistent performance degradation, particularly on videos with temporal inconsistencies such as StableAnimator and CogVideo. Moreover, using SFT for fine-tuning the model results in a marked performance drop compared to our approach, highlighting the essential role of GRPO in enhancing the model’s ability to generalize across various video generation methods. These results demonstrate that the semantic extractor, residual extractor, and temporal reward mechanism work together to enhance the model’s ability to detect both spatial and temporal artifacts in AI-generated videos, yielding the best results when all components are combined.

5 Conclusion

In this paper, we propose **AvatarShield**, a novel multimodal human-centric synthetic video detection framework that integrates GRPO into the training of LLM. To the best of our knowledge, this is the first attempt to introduce GRPO-based reinforcement learning into AI-generated video

detection. By leveraging this innovative training paradigm, we successfully stimulate and enhance the intrinsic reasoning and perceptual abilities of LLM, thereby reducing reliance on costly supervised fine-tuning. Our proposed method achieves state-of-the-art performance across both in-domain and cross-domain evaluation settings, significantly outperforming existing baselines. Notably, the cross-domain experiments, designed to simulate real-world scenarios involving unseen forgery methods, demonstrate the robust generalization capability of AvatarShield. This highlights the practical applicability and resilience of our system in addressing the evolving threats posed by AI-generated video content. Looking ahead, AvatarShield has the potential to contribute broadly across various application domains. These include but are not limited to digital media forensics, social media content moderation, legal and law enforcement investigations, and the protection of personal portrait rights. By providing a scalable and generalizable detection solution, our work lays a solid foundation for building trustworthy AI systems capable of safeguarding visual content authenticity in an increasingly synthetic media landscape.

Limitations: Despite the strong performance of our method, it still has certain limitations. The inference speed of large language models on long video sequences remains relatively slow, which can be solved by using LLM acceleration and pruning methods [77]. Additionally, although our method shows good generalization across existing generation methods, its robustness against future techniques with more subtle artifacts still needs further exploration.

Appendix A Dataset Construction

Our FakeHumanVid dataset is constructed using 9 distinct video generation methods, covering three

major modalities: text-driven, pose-driven, and audio-driven video synthesis. Among them, we employed the official APIs of four production-grade models, namely Kling I2V version 1.6 [2], Hailuo I2V-01 live [66], Wanx I2V version 2.1 [68], and CogVideo-X2 [67], to ensure stable access to their latest functionalities. The remaining five methods, including StableAnimator [5], MimicMotion [6], ControlNeXt [64], Hallo 3 [4], and HelloMeme [65], were reproduced locally using their official open-source code and pretrained weights available on GitHub. This hybrid strategy balances quality and reproducibility, providing a rich variety of video styles. The construction process for each method is described in detail below.

Kling (I2V v1.6) [2]: Kling 1.6, developed by Kuaishou Technology, is an advanced image-to-video generation model. It transforms static images into dynamic 5-second videos at 720p resolution, offering high-quality visual outputs with enhanced motion and semantic understanding. This version introduces significant improvements over its predecessor, Kling 1.5, making it a standout tool for content creators looking to transform static images into dynamic video content.

Hailuo (I2V-01-live) [66]: Hailuo I2V-01 Live is a specialized image-to-video (I2V) model that converts still images into animated video sequences. It maintains consistency across frames while providing smooth motion and precise control over facial expressions and camera movements. This model is specifically trained for Live2D and general animation use cases.

Wanx (I2V v2.1) [68]: Wanx 2.1 is an open-source AI video generation model based on Diffusion Transformer and Wan-VAE. It supports various tasks like text-to-video (T2V), image-to-video (I2V), and more. Wanx 2.1 offers superior performance, multi-tasking capabilities, and consumer-grade GPU compatibility, setting a new standard for video generation.

CogVideo-X2 [67]: CogVideo-X2 is a text-to-video generation model focused on creating more coherent videos aligned with a prompt. It achieves this using several methods, including a 3D variational autoencoder that compresses videos spatially and temporally, improving compression rate and video accuracy.

StableAnimator [5]: StableAnimator is a high-quality identity-preserving human image animation tool. It generates high-fidelity video based

on reference images and pose sequences without post-processing. The model begins by computing image and face embeddings with off-the-shelf extractors and introduces a novel distribution-aware ID Adapter to prevent interference caused by temporal layers while preserving identity via alignment.

MimicMotion [6]: MimicMotion is a high-quality human motion video generation model with confidence-aware pose guidance. Developed by Tencent and Shanghai Jiao Tong University, it can generate detailed and realistic human motion videos from a single pose sequence image, handling various activities like dance, sports, or everyday actions effortlessly.

ControlNeXt [64]: ControlNeXt is a controllable video and image generation model that supports various base models (SD1.5, SDXL, SD3, SVD) and tasks (image/video generation with various conditions). It introduces a lightweight controllable module that reduces trainable parameters by up to 90% compared with ControlNet, achieving faster convergence and outstanding efficiency.

Hallo 3 [4]: Hallo 3 is an open-source portrait animation model developed by Fudan Vision Lab. It uses Diffusion Transformer Networks to generate realistic talking head videos from photos and audio. The model addresses challenges in handling non-frontal perspectives, rendering dynamic objects around the portrait, and generating immersive, realistic backgrounds.

HelloMeme [65]: HelloMeme is an open-source portrait animation model that integrates spatial weaving attention mechanisms to provide high-quality image and video generation. It supports Gradio and ComfyUI interfaces, enabling a wide range of experiments and applications. HelloMeme is designed to generate localized high-fidelity expression-action-consistent images or videos.

Appendix B Answer Analysis

To better understand the interpretive focus of the model during the detection of AI-generated videos, we conduct a linguistic analysis of the most frequent nouns, adjectives, and verbs in its explanations. The resulting word cloud, illustrated in Figure 6, highlights dominant concepts and linguistic signals emphasized by the model. Key terms such as ‘natural’, ‘artifact’, ‘motion’, ‘real’, ‘consistent’, and ‘movement’ suggest that the model

You are a professional video forensic analyst specializing in human motion analysis and forgery detection. Your task is to determine whether a given video is AI-generated content (AIGC) or captured by a real camera. For each case, you are provided with two video inputs:

- Video 1: The original video.
- Video 2: The residual between the VQ-VAE reconstructed video and the original.

The VQ-VAE reconstruction process amplifies diffusion traces and generative artifacts. Analyze both videos in parallel to reveal any discrepancies that indicate forgery.

Core Objective

Identify artifacts and inconsistencies that distinguish AI-generated content from natural recordings through frame-level and temporal analysis.

Analysis Workflow

1. Frame-Level Inspection

- Examine eyes: Check for irregular blink patterns, asymmetric pupils, or missing corneal reflections.
- Analyze hair/texture: Look for unnatural strand groupings, repetitive patterns, or lack of fine gradients.
- Verify text/numbers: Detect character deformities, inconsistent font rendering, or floating glyphs.

2. Motion Analysis

- Evaluate fluid dynamics: Identify viscous-looking liquids, smoke with rigid movement, or fire with looping patterns.
- Study cloth/hair physics: Flag movements violating air resistance principles (e.g., sudden directional changes without wind).
- Track object persistence: Monitor temporal inconsistencies (e.g., disappearing/reappearing items across frames).

3. Lighting Consistency Check

- Map shadow directions: Compare shadows cast by multiple objects in the same scene.
- Validate reflections: Confirm environmental consistency in mirrored surfaces and water ripples.
- Detect HDR anomalies: Identify unrealistic highlight blooming or unnaturally uniform shadow details.

4. Biological Motion Verification

- Audit human kinematics: Check finger joint angles, foot-ground contact during walking, and natural weight shifts.
- Scrutinize facial micro-expressions: Identify missing subtle muscle movements (e.g., asymmetrical eyebrow raises).
- Monitor animal locomotion: Verify biomechanical plausibility in limb/wing movements.

5. Spatial-Temporal Coherence Test

- Track background stability: Detect unexplained shifts in static scene elements.
- Analyze depth of field: Flag focus transitions that contradict physical camera optics.
- Check edge consistency: Identify flickering outlines or unstable object boundaries.

6. Noise/Compression Artifact Analysis

- Profile noise patterns: Differentiate between sensor noise (random) and generative noise (structured).
- Examine compression artifacts: Distinguish blocky MPEG artifacts from AI's frequency-domain inconsistencies.

7. Reconstruction Residual Analysis

- Video 2 represents the residual difference between the VQ-VAE reconstruction and the original video. Based on prior knowledge, genuine videos typically yield larger residuals, whereas AI-generated videos tend to produce smaller residuals. Please use the residual information in Video 2 to support your assessment.

Decision-Making Protocol

- Step 1: Perform modular checks (items 1-6 above) and score anomalies per category.
- Step 2: Cross-validate findings:
 - Hard evidence: Physical law violations (e.g., contradictory shadows) = strong AIGC indicators.
 - Soft evidence: Multiple subtle irregularities (e.g., 3+ minor texture/animation flaws).
- Step 3: Apply confidence grading:
 - Definite AIGC: ≥ 2 hard evidence points.
 - Probable AIGC: 1 hard + ≥ 3 soft evidence points.
 - Inconclusive: Insufficient evidence meeting thresholds.

Fig. 7: Illustrations of our detection system prompt design. We guide the LLM to comprehensively evaluate the authenticity of a video by considering aspects such as frame-level inspection, motion, and lighting.

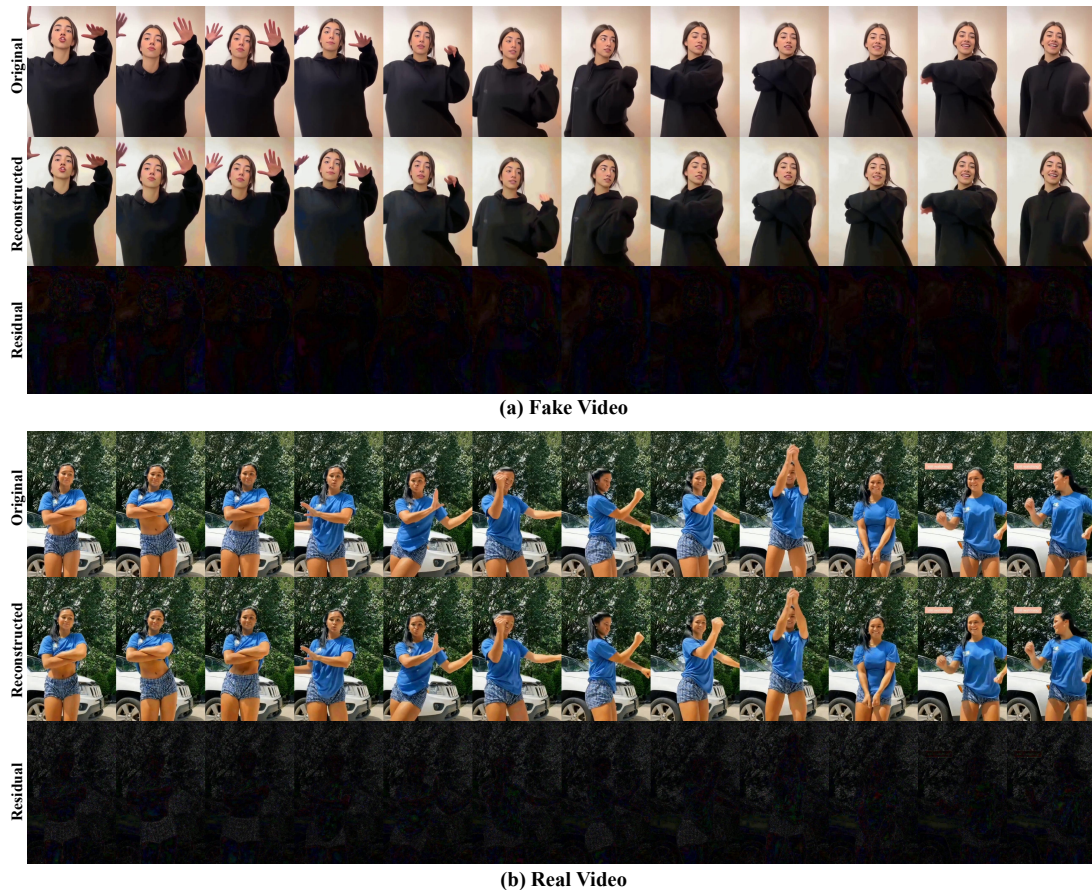


Fig. 8: Visualized residual maps, reconstructed videos produced by VQ-VAE, and original videos of the real and fake videos. We observe that the reconstruction residual artifacts of real videos are significantly more noticeable than those of fake videos, which can serve as a basis for forgery detection.

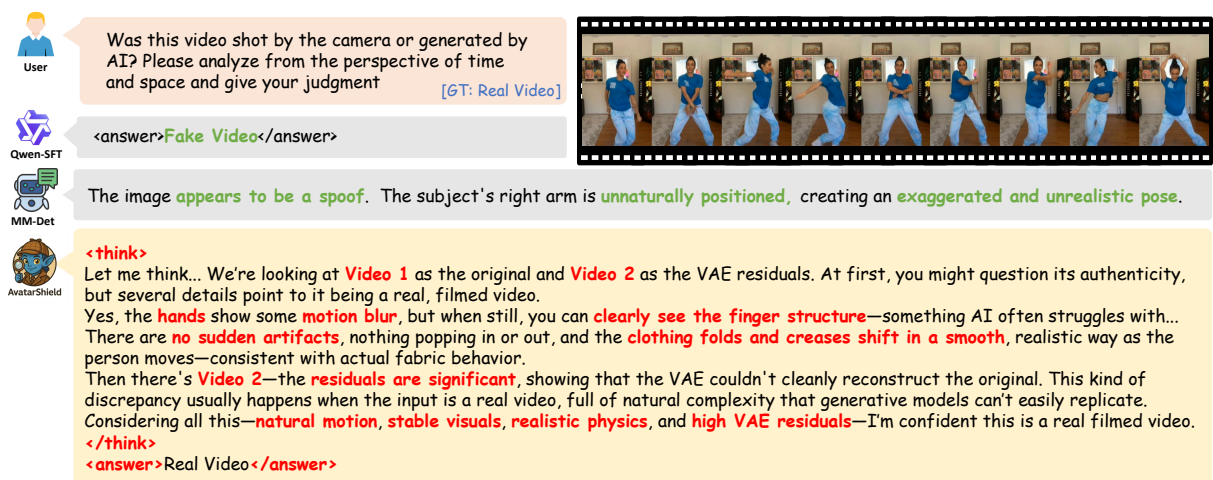


Fig. 9: Comparison results between our method, Qwen-SFT, and MM-Det. Our method is the only model that achieves unified precise detection and video interpretation.

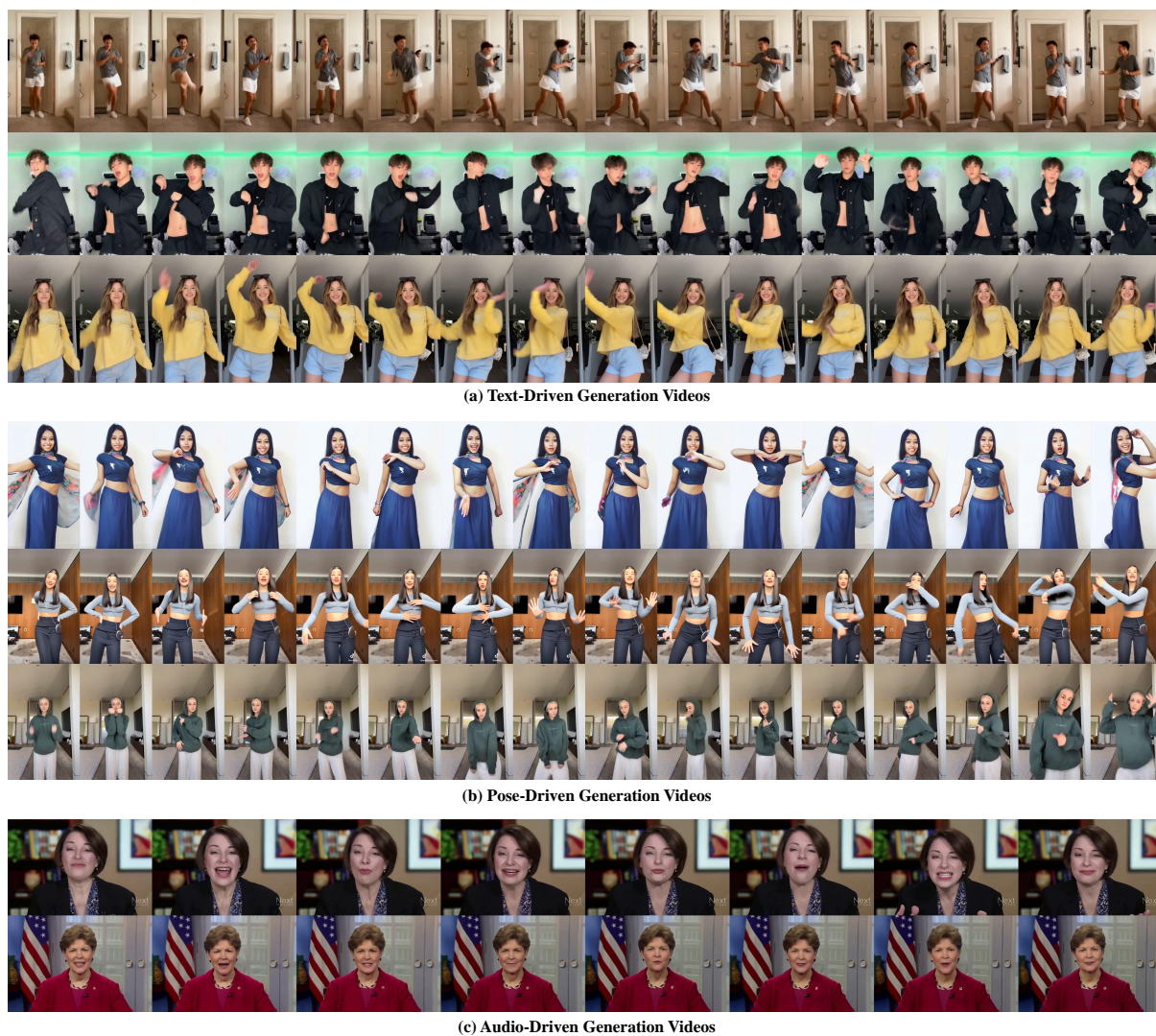


Fig. 10: Sampled results of our constructed FakeHumanVid, including text-driven, pose-driven, and audio-driven generation videos.



User



Is this video a genuine recording captured in the real world, or was it synthetically created by AI?

[GT: Fake Video]

<think>

Let me think... This video features a woman dancing in a modern kitchen. She's wearing a fitted long-sleeve shirt, blue shorts, and white shoes. The kitchen setting includes brown cabinets, sleek countertops, and recessed ceiling lights, giving the impression of a clean, well-lit environment. At first glance, the sequence appears visually appealing and fluid—but a deeper analysis reveals that this is most likely a fake, AI-generated video.

First, let's talk about the **hands**. Throughout the video, the woman's hands are **noticeably blurred**, lacking any clear separation between fingers. Instead of distinct, articulated shapes, the hands appear as smooth, shapeless smears, which is a well-known flaw in AI video generation where the model struggles to resolve detailed extremities under motion.

Next, there's a moment of **waist rotation** during the dance where the torso twists sharply. However, the motion seems **unnaturally exaggerated**, producing a kind of **unsupported anatomical distortion** that would be physically uncomfortable or even impossible in real life. This type of over-rotation without corresponding body mechanics is often seen in generative errors.

The **hair movement** is also suspicious. As she dances, the hair shifts back and forth, but it does so with **uniform, unnatural swaying** that fails to reflect real-world forces like inertia and gravity. The motion lacks the chaos and lag that natural hair would exhibit during such movements.

Additionally, the way her body **interacts with the environment** is off. When she leans on the kitchen counter or places her foot on the floor, the contact appears **visually disconnected**, lacking any realistic compression, shadow, or weight transfer. The figure seems to hover or glide rather than physically engaging with her surroundings.

Finally, the **VAE residuals for this video are minimal**, indicating that the video aligns very closely with the model's latent space. This is typical for AI-generated outputs, where reconstruction is easy because the content itself was synthetically produced.

Combining all these cues—**blurred hands, unnatural joint movement, physics-defying hair, weak environmental interaction, and low residuals**—leads to one clear conclusion: this is a fake video generated by AI.

</think>

<answer>Fake Video</answer>



AvatarShield



User



Was this video filmed with a real camera in the physical world, or is it an artificially generated AI video?

[GT: Fake Video]

<think>

Let me think... This sequence of frames appears to capture a casual dance performed by a young man in an outdoor setting. He's dressed in a black t-shirt, pink shorts, dark sneakers, and a light gray baseball cap worn backward. The location seems like a suburban backyard, with beige siding, white-trimmed windows, and a patio floor. The light conditions suggest late afternoon or early evening, and the overall visual quality appears smooth at first glance.

But as we go frame by frame, several **anomalies** start to emerge that raise strong suspicions of **AI generation**.

First, the **hands** are highly **blurred in multiple frames**, far beyond typical camera motion blur. They lose form entirely, with fingers merging into shapeless patches—this is a frequent limitation of generative models that approximate rapid motion but can't resolve fine extremity detail.

Next, the **arm poses** reveal some unsettling distortions. In several frames, the **arms twist in ways that defy human anatomy**—elbows and wrists are bent at awkward angles, and joint movement doesn't follow natural skeletal constraints. These kinds of deformations are classic symptoms of motion synthesis errors, where the AI miscalculates limb rotation and structure.

Then there's a major inconsistency near the end of the sequence: the **hat suddenly flickers and changes shape** in a single frame. It appears to warp or momentarily vanish, which **violates physical continuity**. No lighting, motion, or natural explanation justifies this behavior—it's an abrupt artifact that suggests instability in the generation process.

Another important clue comes from the **VAE residuals, which show minimal difference from the original video**. This is a strong indicator that the video's content fits well within the latent distribution of the generative model—something we would not expect from real footage, which typically contains more complex texture and motion variability that VAE reconstructions struggle to replicate.

In a genuine video, you'd expect physical consistency, clear body structure, and temporally coherent movement. Here, we get softened detail, unnatural body mechanics, physics-breaking glitches, and low reconstruction error. So when we weigh all these factors—**excessive hand blur, abnormal arm twisting, the sudden hat flicker, and minimal VAE residuals**—the evidence points clearly in one direction: this is an **AI-generated video**.

</think>

<answer>Fake Video</answer>



AvatarShield

Fig. 11: More detection and explanation results of our AvatarShield on text-driven generation videos.



User



Is the video the result of real-world filming, or has it been digitally crafted by artificial intelligence?

[GT: Fake Video]

<think>

Let me think... This video features a man in a suit speaking in front of a wood-paneled wall and multiple American flags. On the surface, the scene appears to resemble a typical political or formal address, but a frame-by-frame inspection reveals several irregularities that strongly suggest this is an AI-generated video.

First, there are noticeable issues with the **face**. Across the frames, the **facial features subtly shift**—the expression, structure, and proportions seem to **morph**, creating the impression that the speaker's **identity fluctuates slightly**. This kind of instability in facial identity is common in deepfake or diffusion-generated content, where the model struggles to maintain consistent high-resolution details across frames.

Second, we observe a problem with the **hands**, particularly at the **bottom of the frames** where a hand appears intermittently. The **fingers look twisted and deformed**, bending in directions that don't align with natural joint structure. The hand appears **detached from believable motion**, and its position shifts unnaturally, suggesting the generation model had difficulty rendering realistic extremities during animated gestures.

A third issue involves a **button-like accessory near the man's collar**. This small detail **flashes in and out of visibility**, sometimes changing in shape or brightness from one frame to the next. In real footage, such an accessory would remain stable unless the lighting or positioning drastically changed—which doesn't appear to be the case here. This inconsistency in minor clothing elements is a known flaw in AI-generated videos where temporal coherence is hard to maintain.

Finally, the **VAE residuals for this video are minimal**, meaning there is little deviation between the original and the VAE's reconstruction. That strongly suggests the video lies comfortably within the latent space of the model—**a telltale sign that the input may have been AI-generated to begin with**.

Taking all of this into account—**shifting facial identity, unnatural hand deformation, flashing accessory artifacts, and minimal VAE residuals**—it becomes clear that this video is not the result of traditional filming. It is most likely an AI-generated video.

</think>

<answer>Fake Video</answer>



AvatarShield



User



Was this scene genuinely captured with a traditional camera, or was it generated through AI algorithms?

[GT: Fake Video]

<think>

Let me think... This video features a woman in formal attire speaking in front of a backdrop that includes an American flag and a government-style setting. At a surface level, everything appears neat and official—but upon closer examination, several subtle yet significant anomalies suggest this is an AI-generated video.

First, throughout the entire frame sequence, **the woman barely blinks**, and when she does, the blinking frequency is unnaturally low and irregular. This is a well-documented issue in synthetic video generation. Many AI models, especially those focused on producing talking-head videos, often neglect to accurately replicate natural blinking rhythms unless explicitly trained on temporal coherence and facial dynamics. Humans blink approximately 15–20 times per minute, often in response to environmental factors or emotional states, and the lack of this behavior in the video feels uncanny.

Second, there is an extreme **lack of movement in the subject's body language**. The woman's head and upper torso remain almost completely static throughout the clip. More notably, there are no hand movements, no gestural emphasis, and no signs of spontaneous posture shifts. In real footage, even highly composed speakers demonstrate micro-movements—slight tilts of the head, repositioning of shoulders, subtle facial expressions, or the occasional use of hands to underscore speech. The absence of such kinetic variability makes the video appear overly controlled and artificial, which is a common characteristic of AI-generated talking-head videos that rely on static templates or constrained motion models.

Next, examining the visual quality, the **hair texture appears unusually smooth and somewhat plasticky**. It lacks the fine, random strand-level detail one would expect in a real-life recording. Additionally, the lighting on both the hair and face is strangely uniform and lacks directional shadows or highlights. This overly even illumination flattens the subject's appearance, diminishing the depth and dimensionality that real-world lighting naturally produces. Simulated lighting environments in AI models often struggle with achieving photorealistic variation, especially in regions like hair or reflective skin surfaces.

Lastly, according to supporting information, **Video 2—the VAE residuals—shows minimal difference** from the original, indicating that the video content aligns closely with the internal distribution of a generative model. In real camera footage, you'd expect a much higher reconstruction error due to complex textures, lighting inconsistencies, and motion nuances.

Putting it all together—**abnormal blinking, unnatural stillness, artificial hair and lighting, and low VAE residuals**—the evidence strongly supports the conclusion that this is an AI-generated video.

</think>

<answer>Fake Video</answer>



AvatarShield

Fig. 12: More detection and explanation results of our AvatarShield on audio-driven generation videos.



User



Can we say this video was shot in the real world with a camera, or does it originate from AI-based generation?

[GT: Fake Video]

<think>

Let me think... This video shows a young man dancing indoors, wearing a maroon sweatshirt with a white printed design. The environment appears to be a warm-lit room, likely a kitchen or dining space, featuring neutral walls and wooden cabinetry. The overall framing and color palette look coherent, and on first impression, the video might seem like a typical social media clip. But as we analyze the details more closely, a number of visual inconsistencies strongly suggest this is an **AI-generated video**.

Let's begin with the **hands**. In nearly every frame, they appear **severely blurred**, far beyond what we would expect from normal motion blur in real camera footage. Even in frames where the hands are relatively still, there's a **lack of anatomical clarity**—the fingers seem **merged together**, and there's no definition between joints. Worse, the hands often look **swollen or puffy**, like a smoothed-out approximation of real human hands. This is a classic shortcoming of diffusion-based video generation, where extremities—especially hands—are notoriously difficult to model correctly under motion.

Now turn to the **hair**. While the subject's hairstyle remains fairly consistent in silhouette, the **movement of the hair is unnaturally soft and blurred**, and in many frames, the **edges of the hair blend into the background**, as if the model struggled to decide where the hair ends and the wall begins. This results in a smeared, fuzzy border that would not occur with a real camera. The **hair motion itself is also off**—instead of following physics-based swaying or bouncing, it shifts in a dull, uniform manner, lacking the randomness and variation that real strands of hair exhibit in motion.

A further anomaly is seen in the **clothing graphics**. The white print on the chest of the sweatshirt **flickers and morphs between frames**. Sometimes it appears cleanly; other times it's warped, cropped, or completely absent. Such **texture instability** is a well-documented issue in frame-by-frame synthesis, where the model fails to preserve consistent visual elements over time.

Moreover, when analyzing **Video 2 (the VAE residuals)**, we notice that the differences are minimal. This low reconstruction error suggests that the original video falls comfortably within the distribution of the generative model's latent space, further reinforcing the idea that the input was synthetically produced.

In sum, **we're seeing blurred and deformed hands, ambiguous and artificial hair behavior**, inconsistent clothing textures, and now, minimal VAE residuals—all compounded by a level of visual smoothness that feels synthetic rather than optical. These signs collectively support a clear conclusion: this is not real footage captured by a camera. It is an **AI-generated video**.

</think>

<answer>Fake Video</answer>



AvatarShield



User



Does this video depict an actual scene recorded by a camera, or is it an AI-generated simulation?

[GT: Fake Video]

<think>

Let me think... At first glance, this video shows a young woman dancing in what looks like a modern, well-lit kitchen or dining area. She's wearing a black crop top, white drawstring pants, and a multi-layered necklace. The scene feels casual and lively—but when examined closely, several **critical visual anomalies** suggest this is an **AI-generated video**.

The first issue is with the **necklace**. Across different frames, the **design of the necklace changes**—sometimes appearing as two layers, sometimes three, with pendants shifting in shape and placement. This kind of **temporal inconsistency** in small, detailed objects is a frequent sign of frame-by-frame generation errors in AI video synthesis.

Next, we notice a **distortion in the arms**. In the later frames, the subject raises her arms in a dancing motion, but the **degree of bending becomes extreme**, causing the limbs to twist in ways that do not align with **normal human anatomy**.

The joints appear to stretch unnaturally, suggesting a poor understanding of skeletal limits by the generative model. Additionally, there's a subtle but disturbing issue with the **face**. While it starts out stable and recognizable, there are moments—particularly in the later frames—where the **facial structure subtly warps**, especially around the eyes and jawline. It gives the impression of a **shifting identity**, a known phenomenon where diffusion-based models fail to preserve consistent facial features throughout motion.

Lastly, the **lighting between the foreground and background** feels mismatched. The woman's body is lit warmly and uniformly, while parts of the background—like the ceiling lights and cabinetry—reflect **inconsistent light direction and intensity**. This disconnect suggests that the subject and environment were not naturally lit together, pointing to possible compositing or synthetic rendering.

Moreover, when analyzing **Video 2 (the VAE residuals)**, we notice that the differences are minimal. This small residual gap suggests that the video fits well within the generative model's latent space, reinforcing the likelihood that this is AI-generated content.

Taken together—**inconsistent jewelry details, unnatural joint deformation, unstable facial identity, mismatched lighting, and now minimal VAE residuals**—this video exhibits multiple indicators of AI generation, despite its initial visual appeal.

</think>

<answer>Fake Video</answer>



AvatarShield

Fig. 13: More detection and explanation results of our AvatarShield on pose-driven generation videos.



User



Is the content of this video rooted in physical reality via camera capture, or was it constructed by an AI model?

[GT: Real Video]

<think>

Let me think... This video captures a person dancing outdoors in front of a white fence and large green trees. She's dressed in a Boston Celtics jersey, denim shorts, and a backward cap, performing a casual dance routine on a gravel surface. At a glance, the video looks vibrant and engaging, but looking deeper, all evidence continues to support that this is a real, camera-recorded video.

First, the **movement of the performer is smooth and natural**. The **dance steps flow seamlessly**, with no visible stiffness or awkward transitions. Every step, bounce, and hand gesture feels grounded in real-world physics, unlike the robotic or segmented motion that often appears in AI-generated content.

Second, the **hair movement is highly realistic**. As the subject turns, jumps, or shifts, the **hair sways in a way that reflects gravity and momentum**, with small variations that suggest true physical simulation rather than synthesized animation. The strands move independently and in sync with body dynamics, which would be difficult to replicate artificially.

Third, the **clothing details reinforce authenticity**. The **creases in the jersey and shorts change naturally** with body motion, stretching and folding in believable ways. The **graphic print** on the shirt remains stable throughout the sequence—no flickering, warping, or inconsistency is visible, which is often a weakness in AI-generated videos that fail to preserve textures over time.

Fourth, the **limbs and extremities are clearly rendered**. While there is some **minor blur in fast movements**, this looks entirely consistent with **natural motion blur** from a real camera, not the smeared, warped distortions that typically appear when AI struggles to generate complex hand or foot movement.

Finally, **Video 2—the VAE residuals—show noticeable differences from the original**, which is exactly what we'd expect from real-world footage. Real videos are rich in detail, lighting variation, and texture complexity, all of which challenge the VAE to reconstruct accurately. The higher residual error confirms that this is likely real content outside the typical training distribution of generative models.

Altogether—fluid body motion, physically accurate hair behavior, consistent clothing texture, clear limb representation, and significant VAE residuals—strongly confirm that this is a real, filmed video, not one generated by AI.

</think>

<answer>Real Video</answer>



AvatarShield



User



Should this video be considered a real-world capture or an artificially generated output from AI?

[GT: Real Video]

<think>

Let me think... This video presents a woman delivering a message in front of an American flag, framed by a painting and floral arrangement. The setting is formal but warm, and at first glance, everything appears stable and natural. Upon closer inspection, the visual and behavioral details strongly support the conclusion that this is a real, filmed video, not AI-generated.

First, the **facial expressions are highly dynamic and natural**. The woman's **mouth movement, brow shifts, and cheek motion** align perfectly with human speech and emotion. There is a clear sense of muscle control in her face—something that AI often struggles to synthesize with subtlety. The **micro-expressions** during speech further support the realism of the footage.

Second, the **head and upper body exhibit normal, spontaneous movement**. As she speaks, her posture subtly shifts, her shoulders rise and settle, and her head gently tilts or nods. These are organic physical behaviors consistent with how a real person would move when communicating.

Third, the **blinking behavior** is another strong indicator. The woman **blinks at a natural frequency**, and the blinks themselves look smooth and realistic—**eyelids fully close and reopen** without jarring motion. This is a detail that many AI-generated videos get wrong, often producing either no blinking at all or unnatural, incomplete eye closure.

Fourth, the **lighting is soft and consistent**, casting gentle shadows that match the position and intensity of the light source. The **reflections and highlights** on the skin, hair, and surroundings all appear realistic, with **no abrupt lighting shifts or inconsistencies** that would suggest digital rendering.

Finally, **Video 2—the VAE residuals—shows noticeable differences from the original**. This is what we expect from a real camera-captured video, where the VAE model struggles to accurately reconstruct the complexity of natural textures, shadows, and facial subtleties. The higher residuals imply that the original contains real-world noise and detail beyond the model's typical latent representation.

With all these observations—**natural facial and body motion, realistic blinking, consistent lighting, and significant VAE residuals**—it is clear that this is a real, camera-recorded video, not AI-generated.

</think>

<answer>Real Video</answer>



AvatarShield

Fig. 14: More detection and explanation results of our AvatarShield on real videos.

References

- [1] Brooks, T., Peebles, B., Holmes, C., DePue, W., Guo, Y., Jing, L., Schmurr, D., Taylor, J., Luhman, T., Luhman, E., *et al.*: Video generation models as world simulators. *OpenAI Blog* **1**, 8 (2024)
- [2] Team, K.: KlingAI: Artificial Intelligence for Enterprises. <https://app.klingai.com/cn/>. Accessed: 2025-04-30 (2025)
- [3] Blattmann, A., Dockhorn, T., Kulal, S., Mendelevitch, D., Kilian, M., Lorenz, D., Levi, Y., English, Z., Voleti, V., Letts, A., *et al.*: Stable video diffusion: Scaling latent video diffusion models to large datasets. *arXiv preprint arXiv:2311.15127* (2023)
- [4] Cui, J., Li, H., Zhan, Y., Shang, H., Cheng, K., Ma, Y., Mu, S., Zhou, H., Wang, J., Zhu, S.: Hallo3: Highly dynamic and realistic portrait image animation with video diffusion transformer (2025)
- [5] Tu, S., Xing, Z., Han, X., Cheng, Z.-Q., Dai, Q., Luo, C., Wu, Z.: Stableanimator: High-quality identity-preserving human image animation. *arXiv preprint arXiv:2411.17697* (2024)
- [6] Zhang, Y., Gu, J., Wang, L.-W., Wang, H., Cheng, J., Zhu, Y., Zou, F.: Mimicmotion: High-quality human motion video generation with confidence-aware pose guidance. *arXiv preprint arXiv:2406.19680* (2024)
- [7] Chen, H., Hong, Y., Huang, Z., Xu, Z., Gu, Z., Li, Y., Lan, J., Zhu, H., Zhang, J., Wang, W., *et al.*: Demamba: Ai-generated video detection on million-scale genvideo benchmark. *arXiv preprint arXiv:2405.19707* (2024)
- [8] Song, X., Guo, X., Zhang, J., Li, Q., Bai, L., Liu, X., Zhai, G., Liu, X.: On learning multi-modal forgery representation for diffusion generated video detection. In: *Advances in Neural Information Processing Systems (NeurIPS)* (2024)
- [9] Kong, C., Luo, A., Bao, P., Li, H., Wan, R., Zheng, Z., Rocha, A., Kot, A.C.: Open-set deepfake detection: A parameter-efficient adaptation method with forgery style mixture. *arXiv preprint arXiv:2408.12791* (2024)
- [10] Kong, C., Luo, A., Bao, P., Yu, Y., Li, H., Zheng, Z., Wang, S., Kot, A.C.: Moe-ffd: Mixture of experts for generalized and parameter-efficient face forgery detection. *arXiv preprint arXiv:2404.08452* (2024)
- [11] Luo, A., Kong, C., Huang, J., Hu, Y., Kang, X., Kot, A.C.: Beyond the prior forgery knowledge: Mining critical clues for general face forgery detection. *IEEE Transactions on Information Forensics and Security* **19**, 1168–1182 (2023)
- [12] Xu, Z., Zhang, X., Li, R., Tang, Z., Huang, Q., Zhang, J.: Fakeshield: Explainable image forgery detection and localization via multi-modal large language models. In: *International Conference on Learning Representations* (2025)
- [13] Huang, Z., Xia, B., Lin, Z., Mou, Z., Yang, W.: Ffaa: Multimodal large language model based explainable open-world face forgery analysis assistant. *arXiv preprint arXiv:2408.10072* (2024)
- [14] Liu, J., Zhang, F., Zhu, J., Sun, E., Zhang, Q., Zha, Z.-J.: Forgerygpt: Multimodal large language model for explainable image forgery detection and localization. *arXiv preprint arXiv:2410.10238* (2024)
- [15] Achiam, J., Adler, S., Agarwal, S., Ahmad, L., Akkaya, I., Aleman, F.L., Almeida, D., Altenschmidt, J., Altman, S., Anadkat, S., *et al.*: Gpt-4 technical report. *arXiv preprint arXiv:2303.08774* (2023)
- [16] Chu, T., Zhai, Y., Yang, J., Tong, S., Xie, S., Schuurmans, D., Le, Q.V., Levine, S., Ma, Y.: Sft memorizes, rl generalizes: A comparative study of foundation model post-training. *arXiv preprint arXiv:2501.17161* (2025)
- [17] Guo, D., Yang, D., Zhang, H., Song, J., Zhang, R., Xu, R., Zhu, Q., Ma, S., Wang, P., Bi, X., *et al.*: Deepseek-r1: Incentivizing reasoning

- capability in llms via reinforcement learning. arXiv preprint arXiv:2501.12948 (2025)
- [18] Ouyang, L., Wu, J., Jiang, X., Almeida, D., Wainwright, C., Mishkin, P., Zhang, C., Agarwal, S., Slama, K., Ray, A., *et al.*: Training language models to follow instructions with human feedback. *Advances in neural information processing systems* **35**, 27730–27744 (2022)
- [19] Zhao, J., Wei, X., Bo, L.: R1-omni: Explainable omni-multimodal emotion recognition with reinforcement learning. arXiv preprint arXiv:2503.05379 (2025)
- [20] Feng, K., Gong, K., Li, B., Guo, Z., Wang, Y., Peng, T., Wang, B., Yue, X.: Video-r1: Reinforcing video reasoning in mllms. arXiv preprint arXiv:2503.21776 (2025)
- [21] Shen, H., Liu, P., Li, J., Fang, C., Ma, Y., Liao, J., Shen, Q., Zhang, Z., Zhao, K., Zhang, Q., *et al.*: Vlm-r1: A stable and generalizable r1-style large vision-language model. arXiv preprint arXiv:2504.07615 (2025)
- [22] Chen, L., Li, L., Zhao, H., Song, Y., Vinci: R1-V: Reinforcing Super Generalization Ability in Vision-Language Models with Less Than \$3. <https://github.com/Deep-Agent/R1-V>. Accessed: 2025-02-02 (2025)
- [23] Tan, H., Ji, Y., Hao, X., Lin, M., Wang, P., Wang, Z., Zhang, S.: Reason-rft: Reinforcement fine-tuning for visual reasoning. arXiv preprint arXiv:2503.20752 (2025)
- [24] Khalid, H., Tariq, S., Kim, M., Woo, S.S.: Fakeavceleb: A novel audio-video multimodal deepfake dataset. arXiv preprint arXiv:2108.05080 (2021)
- [25] Kang, H., Wen, S., Wen, Z., Ye, J., Li, W., Feng, P., Zhou, B., Wang, B., Lin, D., Zhang, L., *et al.*: Legion: Learning to ground and explain for synthetic image detection. arXiv preprint arXiv:2503.15264 (2025)
- [26] Narayan, K., Agarwal, H., Thakral, K., Mittal, S., Vatsa, M., Singh, R.: Df-platter: Multi-face heterogeneous deepfake dataset. In: *Proceedings of the IEEE/CVF Conference on Computer Vision and Pattern Recognition*, pp. 9739–9748 (2023)
- [27] Cai, Z., Ghosh, S., Adatia, A.P., Hayat, M., Dhall, A., Gedeon, T., Stefanov, K.: Avdeepfake1m: A large-scale llm-driven audio-visual deepfake dataset. In: *Proceedings of the 32nd ACM International Conference on Multimedia*, pp. 7414–7423 (2024)
- [28] Zhang, Z., Li, L., Ding, Y., Fan, C.: Flow-guided one-shot talking face generation with a high-resolution audio-visual dataset. In: *Proceedings of the IEEE/CVF Conference on Computer Vision and Pattern Recognition*, pp. 3661–3670 (2021)
- [29] Jafarian, Y., Park, H.S.: Learning high fidelity depths of dressed humans by watching social media dance videos. In: *Proceedings of the IEEE/CVF Conference on Computer Vision and Pattern Recognition (CVPR)*, pp. 12753–12762 (2021)
- [30] Bai, S., Chen, K., Liu, X., Wang, J., Ge, W., Song, S., Dang, K., Wang, P., Wang, S., Tang, J., Zhong, H., Zhu, Y., Yang, M., Li, Z., Wan, J., Wang, P., Ding, W., Fu, Z., Xu, Y., Ye, J., Zhang, X., Xie, T., Cheng, Z., Zhang, H., Yang, Z., Xu, H., Lin, J.: Qwen2.5-vl technical report. arXiv preprint arXiv:2502.13923 (2025)
- [31] Van Den Oord, A., Vinyals, O., *et al.*: Neural discrete representation learning. *Advances in neural information processing systems* **30** (2017)
- [32] Zhong, N., Xu, Y., Li, S., Qian, Z., Zhang, X.: Patchcraft: Exploring texture patch for efficient ai-generated image detection. arXiv preprint arXiv:2311.12397 (2023)
- [33] Zhong, N., Xu, Y., Qian, Z., Zhang, X.: Rich and poor texture contrast: A simple yet effective approach for ai-generated image detection. *CoRR* (2023)
- [34] Zhang, B., Li, S., Feng, G., Qian, Z., Zhang, X.: Patch diffusion: a general module for face manipulation detection. In: *Proceedings of the*

AAAI Conference on Artificial Intelligence, vol. 36, pp. 3243–3251 (2022)

- [35] Yu, X., Chen, K., Zeng, K., Fang, H., Yang, Z., Shang, X., Qi, Y., Zhang, W., Yu, N.: Semgir: Semantic-guided image regeneration based method for ai-generated image detection and attribution. In: Proceedings of the 32nd ACM International Conference on Multimedia, pp. 8480–8488 (2024)
- [36] Fang, Z., Zhao, H., Wei, T., Zhou, W., Wan, M., Wang, Z., Zhang, W., Yu, N.: Uniforensics: Face forgery detection via general facial representation. arXiv preprint arXiv:2407.19079 (2024)
- [37] Salvi, D., Liu, H., Mandelli, S., Bestagini, P., Zhou, W., Zhang, W., Tubaro, S.: A robust approach to multimodal deepfake detection. *Journal of Imaging* **9**(6), 122 (2023)
- [38] Tan, C., Tao, R., Liu, H., Gu, G., Wu, B., Zhao, Y., Wei, Y.: C2p-clip: Injecting category common prompt in clip to enhance generalization in deepfake detection. In: Proceedings of the AAAI Conference on Artificial Intelligence, vol. 39, pp. 7184–7192 (2025)
- [39] Li, Y., Li, Y., Wang, X., Wu, B., Zhou, J., Dong, J.: Texture, shape and order matter: A new transformer design for sequential deepfake detection. In: 2025 IEEE/CVF Winter Conference on Applications of Computer Vision (WACV), pp. 202–211 (2025). IEEE
- [40] Zhu, D., Li, Y., Wu, B., Zhou, J., Wang, Z., Lyu, S.: Hiding faces in plain sight: Defending deepfakes by disrupting face detection. arXiv preprint arXiv:2412.01101 (2024)
- [41] Yan, Z., Wang, J., Wang, Z., Jin, P., Zhang, K.-Y., Chen, S., Yao, T., Ding, S., Wu, B., Yuan, L.: Effort: Efficient orthogonal modeling for generalizable ai-generated image detection. arXiv preprint arXiv:2411.15633 (2024)
- [42] Yang, Z., Chen, R., Yan, Z., Zhang, K.-Y., Fu, X., Wu, S., Shu, X., Yao, T., Yan, J., Ding, S., et al.: All patches matter, more patches better: Enhance ai-generated image detection via panoptic patch learning. arXiv preprint arXiv:2504.01396 (2025)
- [43] Yan, Z., Zhao, Y., Chen, S., Guo, M., Fu, X., Yao, T., Ding, S., Yuan, L.: Generalizing deepfake video detection with plug-and-play: Video-level blending and spatiotemporal adapter tuning. arXiv preprint arXiv:2408.17065 (2024)
- [44] Zhou, J., Li, Y., Wu, B., Li, B., Dong, J., et al.: Freqblender: Enhancing deepfake detection by blending frequency knowledge. *Advances in Neural Information Processing Systems* **37**, 44965–44988 (2024)
- [45] Luo, A., Cai, R., Kong, C., Ju, Y., Kang, X., Huang, J., Life, A.C.K.: Forgery-aware adaptive learning with vision transformer for generalized face forgery detection. *IEEE Transactions on Circuits and Systems for Video Technology* (2024)
- [46] Guo, X., Song, X., Zhang, Y., Liu, X., Liu, X.: Rethinking vision-language model in face forensics: Multi-modal interpretable forged face detector. In: Proceedings of the Computer Vision and Pattern Recognition Conference, pp. 105–116 (2025)
- [47] Narayan, K., VS, V., Patel, V.M.: Facexbench: Evaluating multimodal llms on face understanding. arXiv preprint arXiv:2501.10360 (2025)
- [48] Cui, X., Li, Y., Zhu, D., Zhou, J., Dong, J., Lyu, S.: Forensics adapter: Unleashing clip for generalizable face forgery detection. arXiv preprint arXiv:2411.19715 (2024)
- [49] Li, L., Bao, J., Zhang, T., Yang, H., Chen, D., Wen, F., Guo, B.: Face x-ray for more general face forgery detection. In: Proceedings of the IEEE/CVF Conference on Computer Vision and Pattern Recognition, pp. 5001–5010 (2020)
- [50] Huang, B., Wang, Z., Yang, J., Ai, J., Zou, Q., Wang, Q., Ye, D.: Implicit identity driven deepfake face swapping detection. In: Proceedings of the IEEE/CVF Conference on Computer Vision and Pattern Recognition, pp. 4490–4499 (2023)

- [51] Yan, Z., Zhang, Y., Fan, Y., Wu, B.: Ucf: Uncovering common features for generalizable deepfake detection. In: Proceedings of the IEEE/CVF International Conference on Computer Vision, pp. 22412–22423 (2023)
- [52] Wang, S.-Y., Wang, O., Zhang, R., Owens, A., Efros, A.A.: Cnn-generated images are surprisingly easy to spot...for now. In: CVPR (2020)
- [53] Frank, J., Eisenhofer, T., Schönherr, L., Fischer, A., Kolossa, D., Holz, T.: Leveraging frequency analysis for deep fake image recognition. In: International Conference on Machine Learning, pp. 3247–3258 (2020). PMLR
- [54] Wang, Z., Bao, J., Zhou, W., Wang, W., Hu, H., Chen, H., Li, H.: Dire for diffusion-generated image detection. In: Proceedings of the IEEE/CVF International Conference on Computer Vision, pp. 22445–22455 (2023)
- [55] Yan, S., Li, O., Cai, J., Hao, Y., Jiang, X., Hu, Y., Xie, W.: A sanity check for ai-generated image detection. arXiv preprint arXiv:2406.19435 (2024)
- [56] Ojha, U., Li, Y., Lee, Y.J.: Towards universal fake image detectors that generalize across generative models. In: CVPR (2023)
- [57] Yan, Z., Luo, Y., Lyu, S., Liu, Q., Wu, B.: Transcending forgery specificity with latent space augmentation for generalizable deepfake detection. In: Proceedings of the IEEE/CVF Conference on Computer Vision and Pattern Recognition, pp. 8984–8994 (2024)
- [58] Cao, J., Ma, C., Yao, T., Chen, S., Ding, S., Yang, X.: End-to-end reconstruction-classification learning for face forgery detection. In: Proceedings of the IEEE/CVF Conference on Computer Vision and Pattern Recognition, pp. 4113–4122 (2022)
- [59] Yan, Z., Ye, J., Li, W., Huang, Z., Yuan, S., He, X., Lin, K., He, J., He, C., Yuan, L.: Gpt-imgeval: A comprehensive benchmark for diagnosing gpt4o in image generation. arXiv preprint arXiv:2504.02782 (2025)
- [60] Chen, Y., Yan, Z., Lyu, S., Wu, B.: X2-dfd: A framework for explainable and extendable deepfake detection. arXiv preprint arXiv:2410.06126 (2024)
- [61] Yan, Z., Yao, T., Chen, S., Zhao, Y., Fu, X., Zhu, J., Luo, D., Wang, C., Ding, S., Wu, Y., et al.: Df40: Toward next-generation deepfake detection. arXiv preprint arXiv:2406.13495 (2024)
- [62] Huang, Z., Hu, J., Li, X., He, Y., Zhao, X., Peng, B., Wu, B., Huang, X., Cheng, G.: Sida: Social media image deepfake detection, localization and explanation with large multimodal model (2025)
- [63] Lei, W., Wang, J., Ma, F., Huang, G., Liu, L.: A comprehensive survey on human video generation: Challenges, methods, and insights. arXiv preprint arXiv:2407.08428 (2024)
- [64] Peng, B., Wang, J., Zhang, Y., Li, W., Yang, M.-C., Jia, J.: Controlnext: Powerful and efficient control for image and video generation. arXiv preprint arXiv:2408.06070 (2024)
- [65] Zhang, S., Jiao, N., Li, T., Yang, C., Xue, C., Niu, B., Gao, J.: Hellomeme: Integrating spatial knitting attentions to embed high-level and fidelity-rich conditions in diffusion models. arXiv preprint arXiv:2410.22901 (2024)
- [66] team, H.A.: Hailuo Video. <https://hailuoai.com/video/create>. Accessed: 2025-05-11 (2025)
- [67] Yang, Z., Teng, J., Zheng, W., Ding, M., Huang, S., Xu, J., Yang, Y., Hong, W., Zhang, X., Feng, G., et al.: Cogvideox: Text-to-video diffusion models with an expert transformer. arXiv preprint arXiv:2408.06072 (2024)
- [68] Wang, A., Ai, B., Wen, B., Mao, C., Xie, C.-W., Chen, D., Yu, F., Zhao, H., Yang, J., Zeng, J., et al.: Wan: Open and advanced large-scale video generative models. arXiv preprint arXiv:2503.20314 (2025)
- [69] Chen, Z., Wu, J., Wang, W., Su, W., Chen, G., Xing, S., Zhong, M., Zhang, Q., Zhu, X., Lu, L., et al.: Internvl: Scaling up vision

- foundation models and aligning for generic visual-linguistic tasks. In: Proceedings of the IEEE/CVF Conference on Computer Vision and Pattern Recognition, pp. 24185–24198 (2024)
- [70] Liu, Z., Ning, J., Cao, Y., Wei, Y., Zhang, Z., Lin, S., Hu, H.: Video swin transformer. arXiv preprint arXiv:2106.13230 (2021)
- [71] Guo, X., Liu, X., Ren, Z., Grosz, S., Masi, I., Liu, X.: Hierarchical fine-grained image forgery detection and localization. In: Proceedings of the IEEE/CVF Conference on Computer Vision and Pattern Recognition (CVPR) (2023)
- [72] Song, J., Meng, C., Ermon, S.: Denoising diffusion implicit models. In: International Conference on Learning Representations (ICLR) (2021)
- [73] Radford, A., Kim, J.W., Hallacy, C., Ramesh, A., Goh, G., Agarwal, S., Sastry, G., Askell, A., Mishkin, P., Clark, J., *et al.*: Learning transferable visual models from natural language supervision. In: International Conference on Machine Learning, pp. 8748–8763 (2021). PmLR
- [74] Prajwal, K., Mukhopadhyay, R., Namboodiri, V.P., Jawahar, C.: A lip sync expert is all you need for speech to lip generation in the wild. In: Proceedings of the 28th ACM International Conference on Multimedia, pp. 484–492 (2020)
- [75] Dong, S., Wang, J., Ji, R., Liang, J., Fan, H., Ge, Z.: Implicit identity leakage: The stumbling block to improving deepfake detection generalization. In: Proceedings of the IEEE/CVF Conference on Computer Vision and Pattern Recognition, pp. 3994–4004 (2023)
- [76] Ba, Z., Liu, Q., Liu, Z., Wu, S., Lin, F., Lu, L., Ren, K.: Exposing the deception: Uncovering more forgery clues for deepfake detection. In: Proceedings of the AAAI Conference on Artificial Intelligence, vol. 38, pp. 719–728 (2024)
- [77] Kwon, W., Li, Z., Zhuang, S., Sheng, Y., Zheng, L., Yu, C.H., Gonzalez, J.E., Zhang, H., Stoica, I.: Efficient memory management for large language model serving with pagedat-tention. In: Proceedings of the ACM SIGOPS 29th Symposium on Operating Systems Principles (2023)